(12) **United States Patent**   (10) **Patent No.:**   **US 7,334,211 B1**

Toros et al.   (45) **Date of Patent:**   **Feb. 19, 2008**

(54) **METHOD FOR DESIGNING A CMOS SENSOR USING PARAMETERS**

(75) Inventors: **Zeynep Toros**, Aliso Viejo, CA (US);
Richard Mann, Torrance, CA (US);
Selim Bencuya, Irvine, CA (US)

(73) Assignee: **ESS Technology, Inc.**, Fremont, CA (US)

(*) Notice: Subject to any disclaimer, the term of this patent is extended or adjusted under 35 U.S.C. 154(b) by 554 days.

(21) Appl. No.: **11/029,101**

(22) Filed: **Dec. 30, 2004**

(51) **Int. Cl.**
G06F 17/50   (2006.01)

(52) **U.S. Cl.** **716/19**; 716/11; 716/21

(58) **Field of Classification Search** 716/1, 716/9, 19, 21
See application file for complete search history.

(56)   **References Cited**

U.S. PATENT DOCUMENTS

5,835,141	A	11/1998	Ackland et al.
6,630,701	B1	10/2003	Rhodes
6,809,358	B2	10/2004	Hsieh et al.
6,815,743	B2	11/2004	Rhodes
6,825,878	B1	11/2004	Rhodes
2002/0008767	A1	1/2002	Lee
2003/0193597	A1	10/2003	Fossum et al.
2004/0053436	A1	3/2004	Rhodes
2004/0094784	A1	5/2004	Rhodes et al.
2004/0135209	A1	7/2004	Hsieh et al.
2004/0173799	A1	9/2004	Patrick
2004/0188727	A1	9/2004	Patrick
2007/0187734	A1 *	8/2007	Adkisson et al. 257/293

OTHER PUBLICATIONS

Ikuko Inoue et al. "New LV-BPD (Low Voltage Buried Photo-Diode) for CMOS Imager" IEEE 1999, pp. 883-886.
Abbas El Gamal "Trends in CMOS Image Sensor Technology and Design" International Electron Devices Meeting Digest of Technical Papers, Dec. 2002 consisting of 4 pages.
Pierre Magnan "Detection of Visible Photons in CCD and CMOS: A Comparative View", Nuclear Instruments and Methods in Physics Research A 504 (2003) pp. 199-212.
H. Rhodes et al. "CMOS Imager Technology Shrinks and Image Performance" IEEE 2004, pp. 7-18.
Yasuyuki Endo et al. "4-micron Pixel CMOS Image Sensor With Low Image Lag and High-Temperature Operability", Sensors and Camera Systems for Scientific, Industrial, and Digital Photography Applications IV, SPIE vol. 5017 (2003), pp. 196-204.
Keiji Mabuchi et al., "CMOS Image Sensors Comprised of Floating Diffusion Driving Pixels With Buried Photodiode" IEEE Journal of Solid-State Circuits, vol. 39, No. 12, Dec. 2004, pp. 2408-2416.
U.S. Appl. No. 10/732,583, filed Dec. 10, 2003, entitled "Device and Method for Image Sensing", inventors Selim Bencuya, Jiafu Luo and Richard Mann.
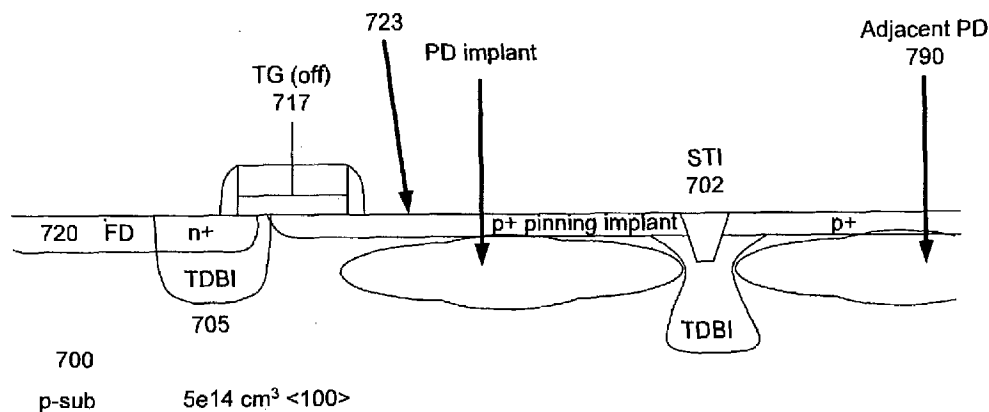
* cited by examiner

Primary Examiner—Thuan Do
(74) *Attorney, Agent, or Firm*—Kenta Suzue; Haynes Beffel & Wolfeld LLP

(57)   **ABSTRACT**

An improved CMOS sensor integrated circuit is disclosed, along with methods of making the circuit and computer readable descriptions of the circuit.

17 Claims, 29 Drawing Sheets
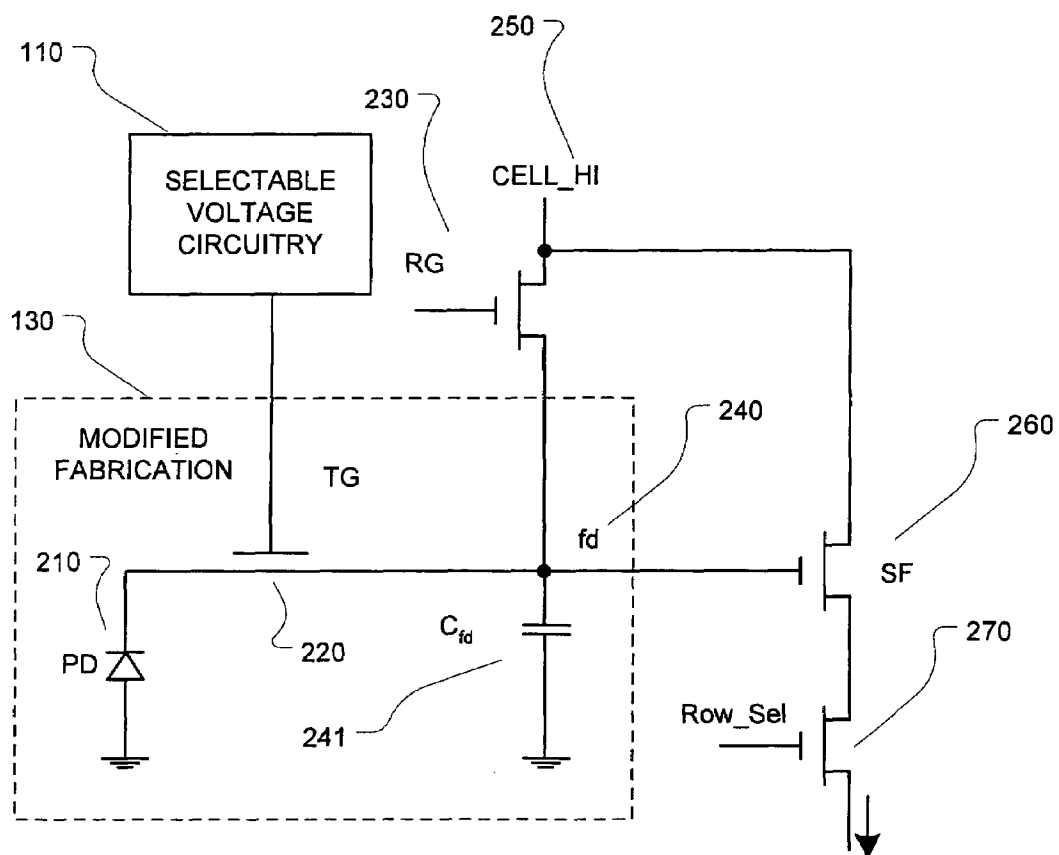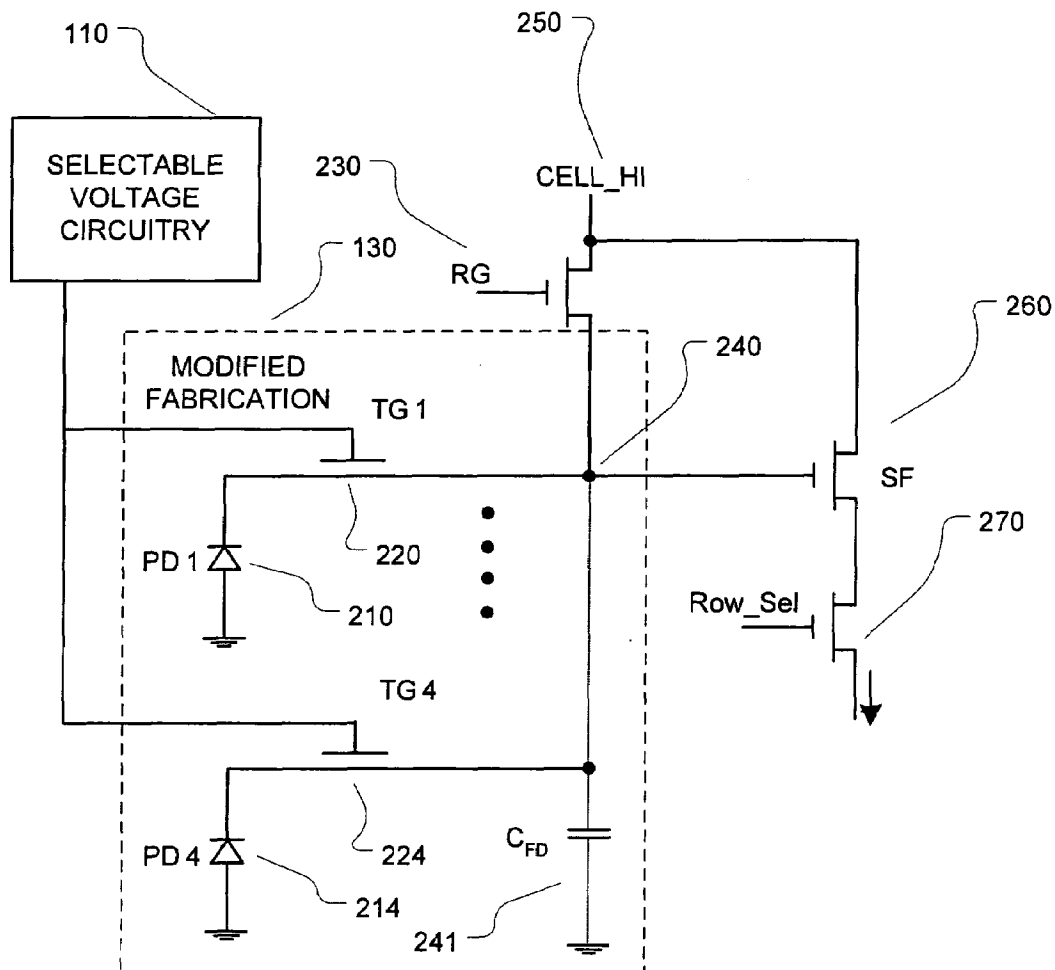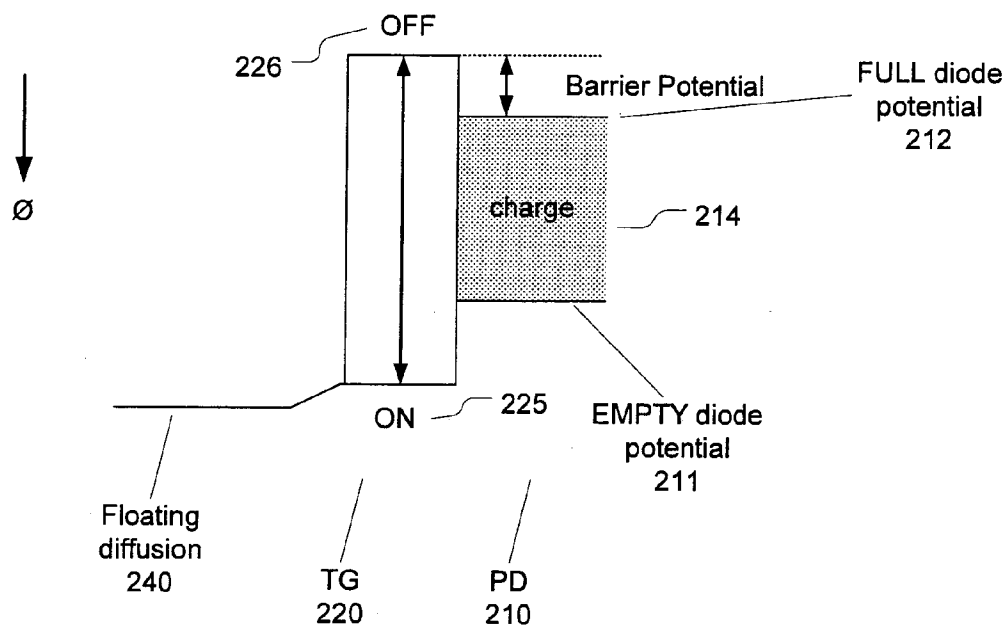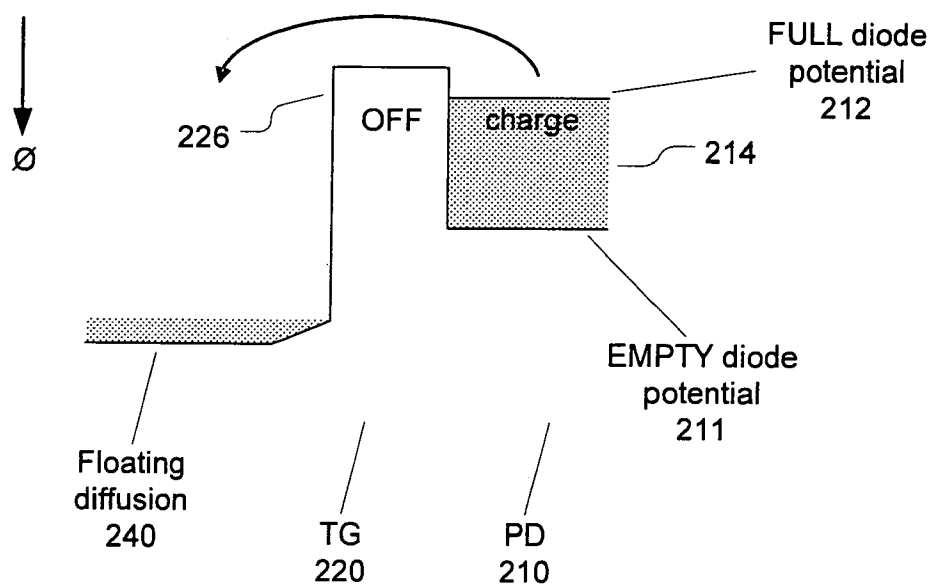**(1 of 29 Drawing Sheet(s) Filed in Color)**

Fig. 1

Fig. 2

Fig. 3

FULL diode potential 212

OFF

charge

226

214

EMPTY diode potential 211

Floating diffusion 240

TG 220

PD 210

Ø

Fig. 4

Fig. 5

Fig. 6

Fig. 7

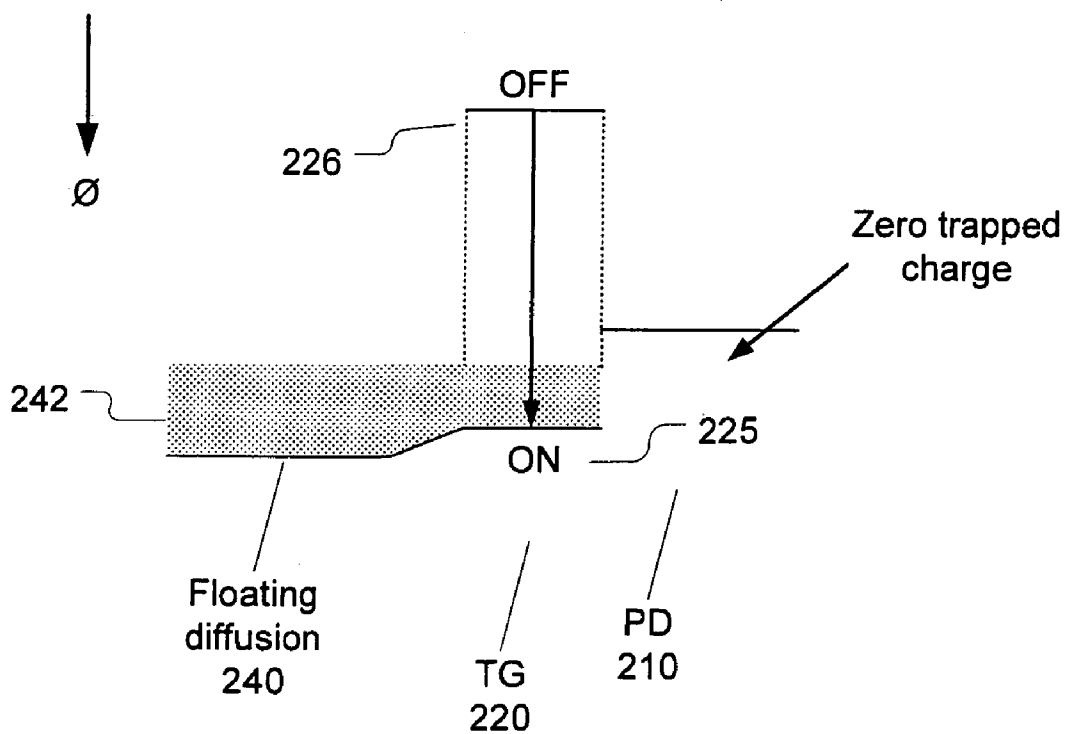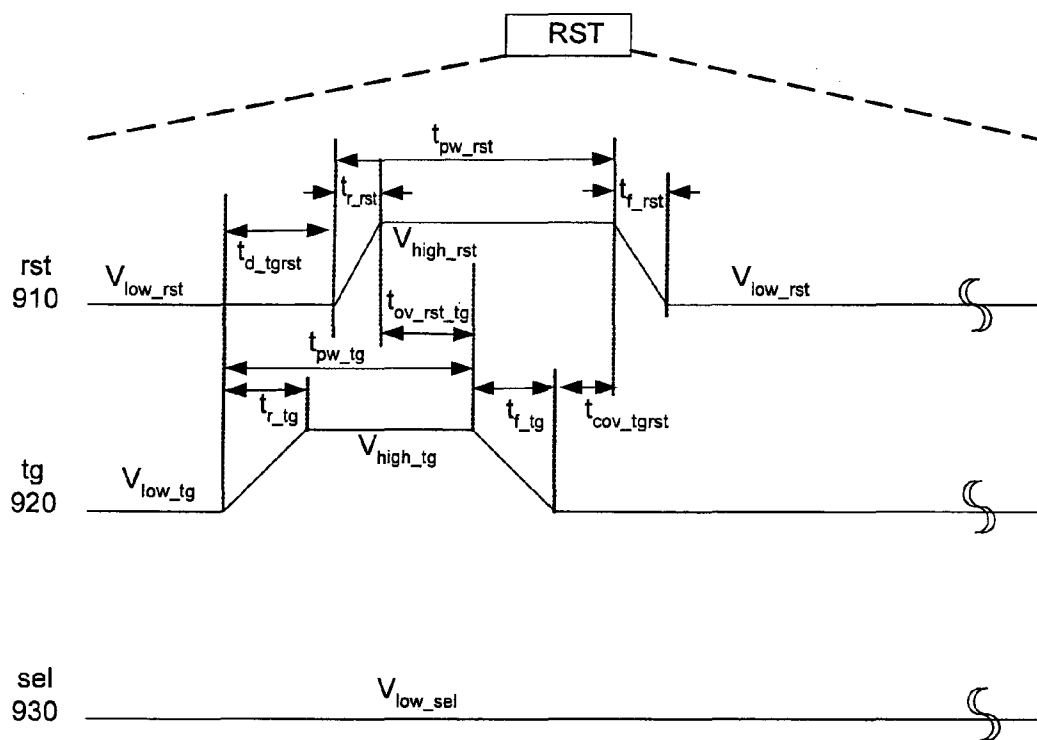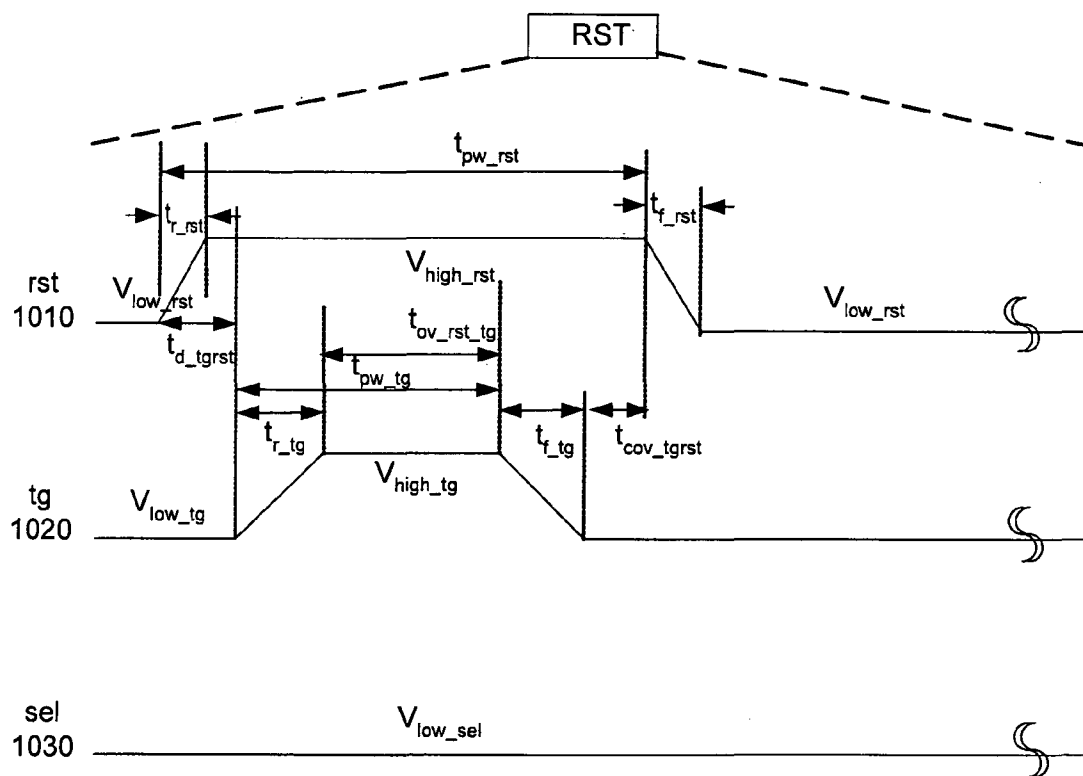**Fig. 8**

Fig. 9

Fig. 10

Fig. 11

Fig. 12

Separation
160

Mask edge for
NMOS p-well
120

Mask edge for
TG p-well
125

p-well for NMOS
708

Transfer Device
Barrier Boron
Implant
705

Fig. 13

PD implant

N-type deep
implant
715   N-type
ring implant
712

RD
730

RG
716

TG
717

p+-pinning
implant
723

Adjacent PD
790

STI
702

0.2um

720

FD   n+

n+

708
Std p - well

TDBI

705

p+

TDBI

p+

p-sub
700

5e14 cm⁻³

<100>

y

x

Fig. 14

Active
Outline →
140

Photodiode
area
143

NMOS
Transistor Gates
145

Separation
160

Charge Transfer
Gate Outline
152

Mask Edge for
NMOS p-well
120

Mask Edge
for TG p-well
125

Fig. 15

diode ring
implant
320

Active
Outline
140

Photodiode
area
143

NMOS
Transistor
Gates
145

Charge
Transfer
Gate Outline
152

Separation
160

Mask Edge for
NMOS p-well
120

Cross-section for the 2-D simulation 1600

Mask Edge
for TG p-well
125

Fig. 16

Fig. 17

Fig. 18

SiO_2
701

702

TDBI

STI

705

p-substrate   700

Fig. 19

Standard p-well
pattern and implant
2000

707

706

702

SiO_2
701

TDBI

STI

705

p-substrate   700
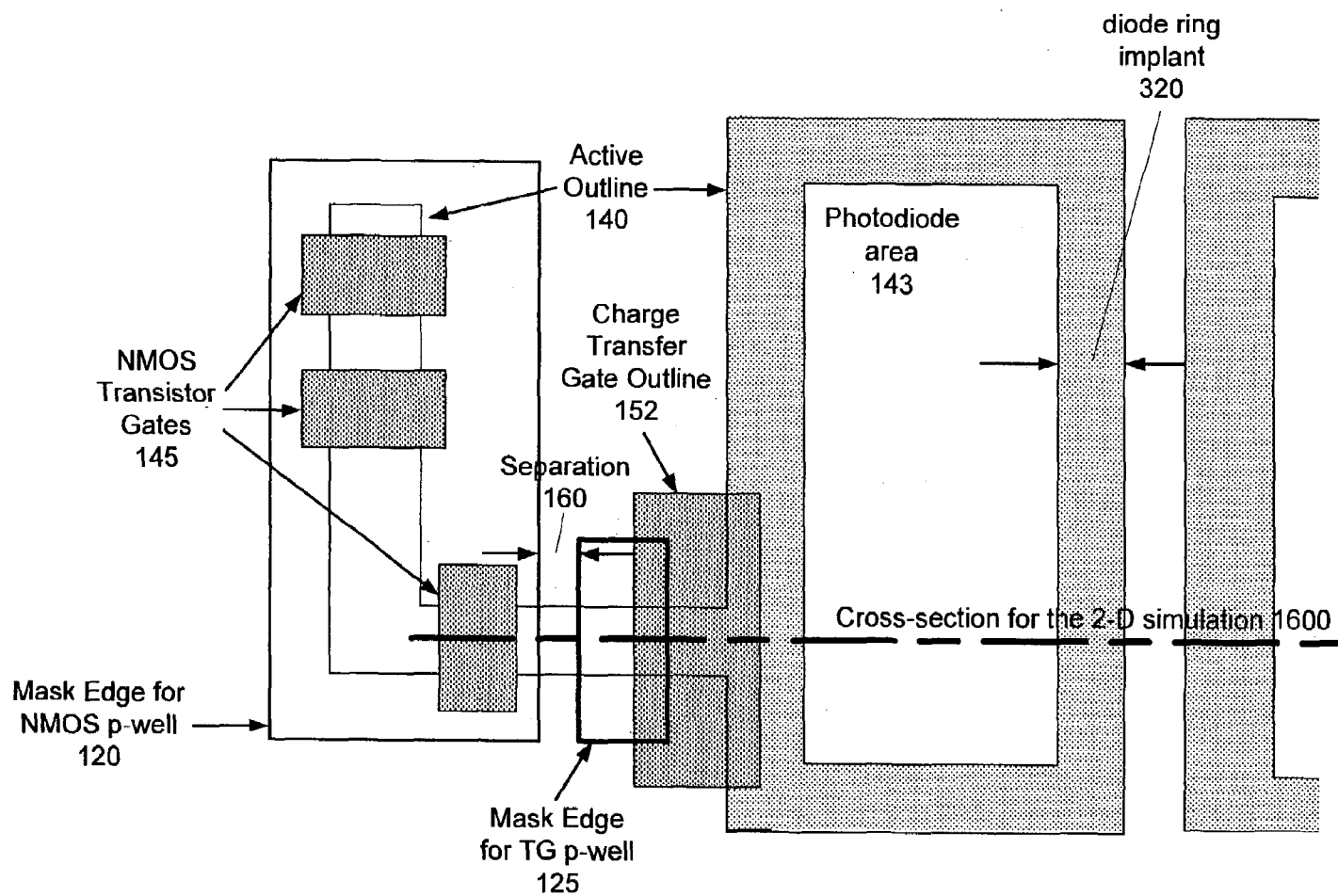
Fig. 20

SiO$_2$ 702

701

p-well   TDBI   STI

                 p-well

708   705   709

p-substrate   700

Fig. 21

Ring_imp
pattern & implant
2200   711

SiO$_2$ 710   702

701

p-well   TDBI   STI

                 p-well

708   705   709

p-substrate   700

Fig. 22

n- type ring implant   n- type ring implant   702   n- type ring implant

SiO_2
701

p-well   TDBI   STI

708   705   712   p-well   709

p-substrate   700

Fig. 23

Diode_ imp
pattern & implant
2400

714

713   n- type ring implant   n- type ring implant   702   n- type ring implant

SiO_2
701

p-well   TDBI   STI

708   705   712   p-well   709

p-substrate   700

Fig. 24

n- type ring   n- type ring   n- type ring
implant   implant   ┌ 702   implant
712 ─┐

SiO₂
701 ─┘   p-well   TDBI   Deep n diode-imp   STI

                                                    p-well
        └ 708   └ 705   └ 715   └ 709
              700
        p-substrate

Fig. 25

Gate oxidation Poly
Deposition and Pattern
2600

                                        n- type ring   n- type ring   n- type ring
                                        implant   implant   ┌ 702   implant
Gate oxide ▨   ⌐ 716   717 ⌐   ▨

701 ─┘   p-well   TDBI   Deep n diode-imp   STI
                            712 ─┘
                                                    p-well
        └ 708   └ 705   └ 715   └ 709
              700
        p-substrate

Fig. 26

nldd pattern and implant
2700

719 ⌇|

⌐718

Gate oxide ⌐716   717 ⌇

701 ⌐

p-well   TDBI

Deep n diode-imp

n- type ring
implant

708 ⌐   705 ⌐   ⌐715   n- type ring   n- type ring
                                     implant   implant

700

p-substrate

p-well   ⌐709

Fig. 27

pldd pattern and implant
2800

⌐722

⌐721|

Gate oxide   ⌐712

701 ⌐   ⌐702

p-well   TDBI

Deep n diode-imp

n- type ring
implant

708 ⌐   705 ⌐   ⌐715   n- type ring   n- type ring
                                     implant   implant

700

p-substrate

p-well   ⌐709

Fig. 28

Idd anneal and spacer
2900

n+ Floating
Diffusion   p+ pinning
                   layer

716   717   723   702   p+ pinning
         724   layer

Gate oxide

701
720   p-well   TDBI   Deep n diode-imp   STI

                                                    p-well   709
708   705   n- type ring
                   implant   715   n- type ring   n- type ring
            700   implant   implant
p-substrate

Fig. 29

n + - S/D pattern   n+ Floating   p+ pinning   p+ pinning
and implant   Diffusion   726   layer   layer
3000

                                                              725
         716   724

Gate oxide

701
720   p-well   TDBI   Deep n diode-imp   STI

                                                    p-well   709
708   705   n- type ring
                   implant   715   n- type ring   n- type ring
            700   implant   implant
p-substrate

Fig. 30

Anneal
3100

n+ Floating
Diffusion

p+ pinning
layer

p+ pinning
layer

716   724   717   723   702

Gate oxide

701

720

p-well   TDBI   Deep n diode-imp   STI

708   705   n- type ring
implant   715   p-well   709

700   n- type ring
implant   n- type ring
implant

p-substrate

Fig. 31

Fig. 32

Adjacent PD
790

STI
702

p+

TDBI

p+ pinning implant

PD implant

723

TG (off)
717

n+

TDBI
705

FD

720

700

p-sub

5e14 cm³ <100>

Fig. 33

EPI THICKNESS
520

Ntype photodiode
550

Surface low
concentration layer
530

P+ Layer of substrate
510

Fig. 34

poly contact on
active channel

RG

TG1

TG2

RG

TG4

SF

Row_Sel

TG3

Row_Sel

Standard p-well

Cell-hi   Output

PD1   PD2

TG1   TG2

Floating
Diffusion

TG3   TG4

PD3   PD4

Transfer Device
Boron Implant
(TDBI)

n-type Ring
Implant

Fig. 35

Fig. 36

METHOD FOR DESIGNING A CMOS SENSOR USING PARAMETERS

REFERENCE TO RELATED APPLICATION

This application is related to the commonly owned U.S. patent applications Ser. No. 11/029,103 (HBES 1012-1), entitled "Method and Apparatus for Varying a CMOS Sensor Control Voltage", by inventors Zeynep Toros, Richard Mann, Selim Bencuya, Sergi Lin and Jiafu Luo; to Ser. No. 11/029,100 (HBES 1013-1), entitled "Method and Apparatus for Removing Electrons from CMOS Sensor Photodetectors", by inventors Zeynep Toros, Richard Mann and Selim Bencuya; to Ser. No. 11/026,460 (HBES 1014-1), entitled "Method and Apparatus for Controlling Charge Transfer in CMOS Sensors with an Implant by the Transfer Gate", by inventors Toros et al.; to Ser. No. 11/026,582 (HBES 1015-1), entitled "Method and Apparatus for Controlling Charge Transfer in CMOS Sensors with a Transfer Gate Work Function", by inventors Toros et al.; to Ser. No. 11/026,278 (HBES 1016-1), entitled "Method and Apparatus for Controlling Charge Transfer in CMOS Sensors with a Graded Transfer Gate Work Function", by inventors Toros et al.; and to Ser. No. 11/029,102 (HBES 1050-1), entitled "Method and Apparatus for Proximate CMOS Pixels" by inventors Toros et al.; all of said applications filed on the same day as this application and all incorporated by reference as if fully set forth herein.

BACKGROUND OF THE INVENTION

1. Field of the Invention

Embodiments are related to image sensors, computer readable descriptions of image sensors, and methods for making mage sensors, and more particularly to such embodiments of CMOS image sensors.

2. Description of Related Art

The active pixel sensor is used in CMOS based imager arrays for a variety of applications. The sensor consists of an array of pixels (rows×columns) with the associated active circuitry on the same chip. Each pixel contains a photosensitive device that senses the incoming light and generates a ΔV difference on a floating node. The readout is accomplished by selecting a row of pixels and reading out each column, either column by column or all columns at the same time. The XY addressable APS is designed for CMOS technology with minor modifications to the process for the pixel while maintaining low-power and lower cost features compared to the CCD technology. Another main advantage of using CMOS process is to have the pixel array with the associated active circuitry on the same chip and save area and cost. Despite all of the benefits of using the CMOS process, the picture quality of the CCD image sensors is still superior to the picture quality of the CMOS APS. One of the main reasons for this difference is that the CMOS process is not suitable to designing a good pixel element, unlike the CCD process which is designed specifically to build pixel elements that result in a high quality picture. Another limitation of the CMOS process is that the operating voltages are low and not flexible as in the CCD technology.

SUMMARY OF THE INVENTION

This innovation describes the process methods and process integration of an active pixel sensor that combines the advantages of both CCD and CMOS technologies. The low noise advantages of a true correlated multiple sampling pixel

(e.g., Correlated Double Sample pixel) are created in a CMOS process with low cost and high performance with minimum impact on existing features and capabilities of the CMOS technology. Disclosed embodiments cover 4T pixel designs, although other protected embodiments cover 5T and other pixel designs.

The design parameters for a CMOS sensor are strongly interdependent. For example, the position and doping of the photodetector, transfer transistor, and the p-type implant by the transfer gate all affect each other. With an appropriate algorithmic flow, the various parameters converge relatively quickly in a reasonable number of iterations.

One embodiment includes: selecting design parameters of a surface p-type region laterally positioned at the photodetector, selecting design parameters of the transfer device, selecting design parameters for a first n-type region and a second n-type region of the photodetector such that the first n-type region is at a first depth range in the integrated circuit and receives the electrons excited by the photons and the second n-type region is at a second depth range such that the first depth range includes depths deeper than the second depth range and the second n-type region is adjacent to the first n-type region and receives the electrons from the first n-type region, selecting design parameters of the p-type region, filling the photodetector with electrons to a maximum capacity, verifying that the maximum capacity of the photodetector meets a design specification of the integrated circuit, verifying that raising the control voltage on the control terminal without exceeding a voltage tolerance of a dielectric transfers the electrons from the photodetector to the corresponding node to be measured and removed.

Other embodiments include a computer algorithm and a set of masks.

BRIEF DESCRIPTION OF THE DRAWINGS

The patent or application file contains at least one drawing executed in color. Copies of this patent or patent application publication with color drawing(s) will be provided by the Office upon request and payment of the necessary fee.

FIG. 1 shows a schematic of a pixel with improved performance.

FIG. 2 shows a schematic of pixels with improved performance that share circuitry.

FIG. 3 shows a sketch of the potential profile in the charge collection and transfer region.

FIG. 4 shows a sketch of charge leakage resulting from a weak barrier when the transfer gate is off.

FIG. 5 shows a sketch of blooming control, where the off voltage of the transfer gate is adjustable to the desired level.

FIG. 6 shows a sketch of the transfer gate is turning on.

FIG. 7 shows a sketch of charge trapping where the transfer gate is on.

FIG. 8 shows a sketch showing that by raising the transfer gate voltage, the barrier is removed, allowing the charge to flow.

FIG. 9 shows a timing diagram of the RST operation to reset the floating diffusion voltage with a positive delay time.

FIG. 10 shows a timing diagram of the RST operation to reset the floating diffusion voltage with a negative delay time.

FIG. 11 shows a timing diagram of the RO (readout) operation to read out the charge, where the SEL (select) signal is turned low after the RST (reset) level is sampled, and the SEL signal is turned high again to sample the signal level.

FIG. **12** shows a timing diagram of the RO operation to read out the charge, where the SEL signal is kept high until the transfer gate voltage is turned low.

FIG. **13** is a cross-sectional schematic of a pixel with a separation between a typical p-well and the transfer device barrier boron p-well.

FIG. **14** is a cross-sectional schematic of a pixel with a separation between the transfer device barrier implant and the reset transistor p-well implant (in this example, with a separation of about 0.3 um-0.5 um), and an overlap of the transfer device barrier implant with the transfer gate (in this example, with an overlap of about 0.2 um).

FIG. **15** is a plan view schematic of a pixel with a separation between the transfer device barrier implant and the reset transistor p-well implant, and an overlap of the transfer device barrier implant with the transfer gate.

FIG. **16** is a plan view schematic of a pixel with an n-type diode ring implant and showing the cross-section for the 2D simulation.

FIG. **17** illustrates part of a pixel fabrication process and shows a cross-sectional view of a pixel with shallow trench isolation.

FIG. **18** illustrates part of a pixel fabrication process and shows the patterning and implantation of the transfer device barrier implant.

FIG. **19** illustrates part of a pixel fabrication process and shows the transfer device barrier implant.

FIG. **20** illustrates part of a pixel fabrication process and shows the patterning and implantation of a typical p-well implant.

FIG. **21** illustrates part of a pixel fabrication process and shows the p-well implant for the signal and reset transistors and isolation of neighboring photodiodes.

FIG. **22** illustrates part of a pixel fabrication process and shows the patterning and implantation of the photodiode ring implant.

FIG. **23** illustrates part of a pixel fabrication process and shows the photodiode ring implant.

FIG. **24** illustrates part of a pixel fabrication process and shows the patterning and implantation of the photodiode deep implant.

FIG. **25** illustrates part of a pixel fabrication process and shows the photodiode deep implant.

FIG. **26** illustrates part of a pixel fabrication process and shows the patterning and growth of the gate oxide and patterning and deposition of the polysilicon gates.

FIG. **27** illustrates part of a pixel fabrication process and shows the patterning and implantation of the nldd, or floating node.

FIG. **28** illustrates part of a pixel fabrication process and shows the patterning and implantation of the pldd, or pinning implant.

FIG. **29** illustrates part of a pixel fabrication process and shows annealing and the growth of the transistor spacers.

FIG. **30** illustrates part of a pixel fabrication process and shows the patterning and implantation of the sources and drains of the transistors.

FIG. **31** illustrates part of a pixel fabrication process and shows the annealing.

FIG. **32** shows a simulation of a cross-section a pixel with the reset transistor, transfer gate, and photodiode.

FIG. **33** is a cross-sectional schematic of a pixel with a p-type polysilicon gate for the transfer gate.

FIG. **34** is a cross-sectional schematic of a photodetector of a pixel showing the p+ epitaxial layer.

FIG. **35** is an example layout of several pixels that share circuitry such as the floating node, reset transistor, and signal transistors.

FIG. **36** is an exemplary computer apparatus and computer code medium.

DETAILED DESCRIPTION

The pixel as illustrated in FIG. **1** is designed to overcome limitations of the CMOS process and achieve good picture quality levels that are comparable to CCD sensors.

The pixel consists of a pinned photodiode (PD) **210** as light sensing element, a transfer gate (TG) **220**, a floating diffusion **240** (and associated capacitance **241**), a MOSFET as reset transistor **230**, a second MOSFET as source follower **260**, and a third MOSFET as row select transistor **210**. The devices which have undergone modified fabrication **130** according to some embodiments include the pinned photodiode (PD) **210**, the transfer gate (TG) **220**, and the floating diffusion **240**.

FIG. **1** also shows selectable voltage circuitry **110** coupled to the transfer gate **220**. One current-carrying terminal of the reset transistor **230** is coupled to the floating diffusion **240** and another current-carrying terminal of the reset transistor **230** is coupled to a current-carrying terminal of the source follower **260**.

The pixel is designed to be built with the CMOS process with additional implantation steps to improve the performance. Only modest positive biasing voltages are required which can easily be provided by a CMOS process without the need for special high voltage devices. The process modifications are in the pixel array and therefore the rest of the on-chip active circuitry need not be affected. Since the pixel uses the same operating voltages, the readout operation, timing, digital control block and the analog signal chain remain the same. The pixel is a 3 MOSFET+1 transfer gate pixel with a pinned photodiode as the light sensing element.

Charge remaining in the PD from the previous frame is called lag. Lag is usually caused by incomplete charge transfer. Incomplete charge transfer occurs mostly due to one or more of:

1) Charge is trapped in the PD because of too large of a barrier between the ON gate and the PD, and

2) In charge injection devices (such as CID imagers), the charge reset occurs by turning the gates off and injecting the charge to the substrate. But, when the gates turn on again, some of this charge may return to the potential well before recombining, resulting in image lag.

The latter cause "2)" is not the case for pixels which do not use the substrate for the charge reset. The PD and transfer region should be designed very carefully to avoid the former cause "1)".

Two effects of lag are that charge is lost from the original frame signal (distorting the current image), and charge is added to the next frame (distorting the next image). Therefore, image lag should be eliminated completely or at least as much as possible.

To eliminate the image lag completely, the CMOS process flow is modified in the pixel area. FIG. **14** illustrates the cross-sectional view of the charge transfer in the pixel that is separated from the adjacent pixel by shallow trench isolation (STI) **702**. The transfer gate **717** is a true gate structure that is placed between the pinned photodiode **712**, **715** and the n-type floating diffusion **720**. The purpose of the transfer gate **717** is:

5

a) to keep the integrated charge in the PD **712, 715** separated from the floating diffusion **720** during charge integration period,

b) to perform complete charge transfer during charge readout by turning transfer gate **717** on, and

c) global reset; electronically resetting the pixels by turning both the transfer gate **717** and reset gate **716** on.

Additional implants help to perform a complete charge transfer:

1) An additional p-type implant **705**, such as a lighter boron doping implant (also called "transfer device barrier Boron implant").

2) A deep n-type photodiode implant **715** (e.g., low dose)

3) A shallow n-type photodiode implant **712** (e.g., ring shaped and high dose).

A fourth implant can also be used to improve performance by adjusting the work function of the transfer device gate **717** to be "graded" from n-type where it overlaps the sense node **720** drain to more p-type where it overlaps the n-type photodiode **712, 715**.

The high performance and low cost of this pixel innovation is also realized through the optimum use and placement of process layers and implants in the baseline CMOS process. Specifically, the p-well for formation of NMOS devices in a CMOS process is employed to provide isolation between pixels. In addition, the p-well provides isolation from the traps and surface states associated with the STI which is used in submicron CMOS. This isolation is used for the integrated photodiode to achieve low dark currents more typical of a CCD device. The PLDD implant is employed to provide junction isolation for dark current reduction from the surface states in the diode.

The transfer device Boron implant (TDBI) helps the TG turn on more easily, and therefore improves the charge transfer. The deep n-implant and n-type ring implant in the PD are both used to adjust the PD capacitance as well as charge transfer operation by introducing a potential gradient that helps the charge move towards the floating diffusion when the TG is turned ON.

By optimizing the pixel as described above, the amount of the charge than can be transferred completely is maximized. Since the floating diffusion potential can be read out before and after charge transfer, the noise level can be reduced by correlated double sampling. Therefore, the dynamic range improves significantly, and image-lag is eliminated. The pixel described in this innovation is comparable to CCD pixels and will result in good picture quality comparable to CCD sensors.

Advantages:

1) Reduced dark current noise: Dark current is one of the important contributors to the output noise. The significant component of the dark current is generated at silicon/silicon dioxide interface. Pinned photodiode will reduce the dark current generation significantly by keeping the surface accumulated with holes. A transfer gate with an appropriate work function, such as p-type polysilicon, reduces dark current under the transfer gate and attracts holes to the region by the transfer gate.

2) Reduced kTC noise: The design of the pixel with the transfer gate enables true correlated double sampling at the output. Therefore the noise that is generated at the output amplifier can be eliminated. The output amplifier becomes very much like a CCD sensor output.

3) Higher signal level: The additional n-type photodiode implants are intended to maximize the capacitance of the PD, and still perform complete charge transfer during readout. The pixel ring implant even increases capacitance in the

6

region between the deep implant and the nearby STI region which has been implanted with p-type dopants.

4) Increased dynamic range: Optimizing the PD capacitance and reducing the output amplifier noise maximizes the dynamic range.

5) The same pixel can be used in shared architecture. (FIG. **2**.) Sharing the SF **260**, RG **230** and Row_Sel **270** transistors increases the fill factor of the pixel. Higher dynamic range and signal-to-noise ratio are achieved.

6) A CMOS pixel sensor is designed to achieve good picture quality associated with CCD image sensors while maintaining

a) low-power

b) low-cost and

c) On chip active circuitry integration features of the CMOS technology.

However, these advantages are accompanied by the addition of extra implant steps to the CMOS process to build the charge transfer device to achieve complete charge transfer.

FIGS. **3-8** show the behavior of the transfer gate. The phi symbol indicates potential increasing in the downward direction of the arrow. Ideally, when the TG **220** is OFF, charge should be collected in the pinned PD **210**. The difference between the full diode potential **212** and empty diode potential **211** determines the charge collection capacity of the pixel. FIG. **3** also shows the collected charge **214**, the barrier height **213** between the collected charge **214** and the transfer gate off potential **226**. This value can be optimized by varying the n-type PD implant, and the TDBI implant.

If the TDBI concentration is too low, then the OFF TG **226** cannot provide enough of a barrier for electrons **214** collected in the PD **210** resulting in a constant leakage into the floating diffusion region **240**. The potential profile of the charge leakage is shown in FIG. **4**. Constant leakage is not desirable and should be avoided. The TG **220** becomes useless and cannot isolate the charge **214** from the FD region **240** during charge integration. The pixel becomes like a 3 transistor pixel. Therefore, the TDBI dose and energy should be selected very carefully to avoid constant charge leakage from the PD **210** to the FD **240** to make sure that the pixel does have enough charge capacity. The dynamic range and signal to noise ratio depend on this signal.

In case of a very bright light, the PD can get saturated and excess charge is going to flow over the OFF TG (FIG. **5**). This is not the same as charge leakage. The TG **220** acts like a blooming control device. The OFF gate voltage can be set to an intermediate value (shown as multiple values **226**) during charge integration for blooming control. Excess charge **242** is drained to the FD, and removed by turning the RG on. Setting the TG OFF voltage to an intermediate value (somewhere between OFF and ON states) essentially controls the signal capacity of the pixel. The highest capacity is obtained with the most negative TG voltage. Intermediate levels reduce the signal, and therefore can be used as blooming control.

The TDBI concentration should be optimized such that while the TG is OFF, the barrier under the TG should provide enough barrier for the charge integrated in the PD. On the other hand, when the TG turns ON, this barrier should disappear completely so that the charge can be transferred.

FIGS. **6** and **7** show the 2D potential profile of the charge transfer area with the TG turning ON **225**. Because of the overly strong TDBI concentration, there is some charge trapped **214** in the PD **210**, as shown in FIG. **7**. This charge causes image lag and is not desired. The pixel should be

designed so that no charge gets trapped in the PD after charge transfer is finished. The need to manage the charge transfer barrier at the proper level is the most difficult aspect of the robust design of the charge transfer device. It is classically difficult to insure a high barrier with no leakage in the off **226** or NO TRANSFER state while assuring the complete transfer of a large amount of charge in the on **225** or transfer state.

In our innovation, the manufacturing and performance window of operation of the pixel is increased by using elevated voltages on the transfer gate. Thus even if there is some residual charge in the PD, by raising the TG voltage even further, this charge can be transferred from the PD to the FD (FIG. **8**). Since the channel potential rises under the transfer gate, the maximum absolute voltage of the transfer gate can be safely increased without creating a high electric field across the gate oxide dielectric materials. The use of higher voltages on the transfer gate is anticipated in the device design, resulting in a strong barrier to charge transfer in the off state which is forced down by a larger voltage on the transfer gate during transfer. In this manner the effective threshold of the transfer device is sufficient to block unwanted charge transfer in the off state. The threshold of the device will vary in manufacture and thus the minimum gate voltage to assure adequate charge transfer will have process variation. Use of a transfer gate voltage which is above the maximum required will insure that the transfer is always complete.

The charge pump should be designed to provide at least one VT above the supply voltage. Higher TG voltage is safe to use since this gate operates with strong backbias. In our innovation an adjustable voltage pulse is provided to the transfer gate in which the maximum applied voltage and the rise and fall times of the transfer gate voltage pulse can be adjusted. On chip adjustment through a DAC is provided to allow testing of the charge transfer properties at a range of voltages. In this manner the needed manufacturing margin for complete charge transfer in product operation can be verified.

After carefully optimizing the TG structure to obtain complete charge transfer, and the PD to achieve desired signal level, the switching time of the TG should also be considered. When the TG switches from ON to OFF, charge can spill back into the PD especially if this gate is turned OFF too quickly. Therefore, enough time should be allowed for this gate to turn off. This time can be in the range of 50 ns to 150 ns.

While the deep n-type diode implant mainly determines the collection depth of the electrons, and the PD capacity, the shallower n-type ring implant in the PD is used to increase the capacity around the edges of the PD. The main purpose of the shallow implant other than contributing to the PD capacity, is to provide a potential gradient toward the TG for the electrons when this gate is turned ON. The three sides of the ring structure neighboring the STI utilize the edges and improve the signal capacity. The side that is adjacent to the poly-gate shifts the potential maximum towards the FD when the TG is turned on and introduces a potential gradient from the center of the PD towards the TG edge of the PD, and acting like a channel for the electrons to flow from the PD over to the FD region. Otherwise, it is much more difficult to transfer the integrated charge completely to the PD, and avoid image lag. The potential gradient also helps the transfer time. Because of this gradient, the electrons move faster to the floating diffusion node, and the time for the charge transfer is reduced significantly. Sample ring implant dose and energy are 8e11, 150 keV.

The TDBI does not extend under the TG completely. Rather, the TDBI extends, for example, by about 0.2 um. These three implants—TDBI, deep n-type diode implant, and the shallow ring-implant—and the TG length are optimized and laid out so that whole range of the supply voltage can be used to store and transfer the charge. The threshold voltage of this gate is reduced so that the charge transfer occurs under this gate very close to the surface. When the gate is turned on, the charge flows from the deep n-diode region to the surface where the shallow n-region is. The TDBI barrier disappears completely under the TG and the charge flows from the shallow n-region into the FD.

Even though charge transfer occurs under the TG at the p-well edge very close to the surface, charge integration takes place in the PD with this gate turned OFF. The collection depth is determined by the deep n-type implant. As more charge gets collected in the PD, the potential maximum in the silicon moves closer to silicon/dioxide interface. The deeper the n-implant goes, the more the PD capacity. Deeper implants also provide a more favorable electric field implant for the collection of red light. The tail of the potential profile is also important. If the junction is too abrupt, the collection of the electrons due to red light becomes more difficult. Therefore, the junction depth is adjusted, for example, to about 1.5 um for this structure. While the shallow n-type ring implant better utilizes edges of the PD, and provides a potential gradient for the charge to transfer close to the silicon surface, the deep n-type implant is used to have enough PD capacity and charge collection depth. The implant dose and energy in one embodiment are about 1e12 and 300 keV for this design.

Red light collection and overall pixel capacity are also optimized by building the device on an epitaxial substrate. An P epi layer of, for example, about 5E14 concentration with a thickness of 4 to 5 microns is optimal in one case. The electric field from the P+ substrates concentration of boron helps to reflect photoelectrons towards the surface for collection by the photodiode.

For this structure, the parameters are boron with dose and energy in the range of 1.75e12, 50 keV and 1.2e13, 200 keV. The best doping levels can be optimized based upon consideration of additional process details such as starting material doping level and the exact thermal cycles of the process.

Timing:

The pixel operation consists of the basic three functions:

1) Resetting the floating diffusion voltage (RST) FIGS. **9** and **10**.

FIGS. **9** and **10** show a timing diagram of the RST operation to reset the floating diffusion voltage. FIG. **9** shows the reset with a positive delay time and FIG. **10** shows the reset with a negative delay time. The sel voltage remains at V_{low_sel}. The tg voltage rises from V_{low_tg} to V_{high_tg} over a time of t_{r_tg}, and then falls back to V_{low_tg} over a time of t_{f_tg}. The rst voltage rises from V_{low_rst} to V_{high_rst} over a time of t_{r_rst}, and then falls back to V_{low_rst} over a time of t_{f_rst}.

The time t_{pw_rst} begins when the rst voltage begins to rise from V_{low_rst} to V_{high_rst}, and ends when the rst voltage begins to fall from V_{high_rst} to V_{low_rst}. The time t_{pw_tg} begins when the tg voltage begins to rise from V_{low_tg} to V_{high_tg}, and ends when the tg voltage begins to fall from V_{high_tg} to V_{low_tg}. The time t_{cov_tgrst} begins when the tg voltage has fallen from V_{high_tg} to V_{low_tg}, and ends when the rst voltage begins to fall from V_{high_rst} to V_{low_rst}.

In FIG. **9**, there is a positive delay time of t_{d_tgrst} from the time when the tg voltage begins to rise from V_{low_tg} to

V_{high_tg}, to the time when the rst voltage begins to rise from V_{low_rst} to V_{high_rst}. In FIG. **10**, there is a negative delay time with a magnitude of t_{d_tgrst} from the time when the rst voltage begins to rise from V_{low_rst} to V_{high_rst} to the time when the tg voltage begins to rise from V_{low_tg} to V_{high_tg}.

The time overlap of the rst voltage being at the voltage V_{high_rst} and the tg voltage being at the voltage V_{high_tg} is the time $t_{ov\_rst\_tg}$. In FIG. **9**, the rst voltage rises from V_{low_rst} to V_{high_rst} after the tg voltage rises from V_{low_tg} to V_{high_tg}, and the tg voltage falls from V_{high_tg} to V_{low_tg} before the rst voltage falls from V_{high_rst} to V_{low_rst}. Thus in FIG. **9**, the time $t_{ov\_rst\_tg}$ begins after the rst voltage has risen from V_{low_rst} to V_{high_rst} and ends when the tg voltage begins to fall from V_{high_tg} to V_{low_tg}. In FIG. **10**, the tg voltage rises from V_{low_tg} to V_{high_tg} after the rst voltage rises from V_{low_rst} to V_{high_rst}, and the tg voltage falls from V_{high_tg} to V_{low_tg} before the voltage of rst falls from V_{high_rst} to V_{low_rst}. Thus in FIG. **10**, the time $t_{ov\_rst\_tg}$ begins after the tg voltage has risen from V_{low_tg} to V_{high_tg} and ends when the tg voltage begins to fall from V_{high_tg} to V_{low_tg}.

2) Charge integration in the photodiode (INT)

3) Charge readout (RO) FIGS. **11** and **12**.

FIGS. **11** and **12** show a timing diagram of the RO (readout) operation to read out the charge. In FIG. **11**, the SEL (select) signal is turned low after the RST (reset) level is sampled, and the SEL signal is turned high again to sample the signal level. In FIG. **12**, the SEL signal is kept high until after the transfer gate voltage is turned low.

The rst voltage rises from V_{low_rst} to V_{high_rst} over a time of t_{r_rst}. In response, the fd voltage rises to $V_{cell\_hi} - V_T'$ (for example, CELL_HI **250** on FIG. **1** minus a threshold voltage). The rst voltage then falls back to V_{low_rst} over a time of t_{f_rst}. In response, the fd voltage falls slightly due to gate coupling. The time t_{pw_rst} begins when the rst voltage begins to rise from V_{low_rst} to V_{high_rst}, and ends when the rst voltage begins to fall from V_{high_rst} to V_{low_rst}.

After a time delay of t_{gap_1} after the rst voltage has fallen back to V_{low_rst}, the sel voltage begins to rise from V_{low_sel}. The sel voltage rises from V_{low_sel} to V_{high_sel} over a time of t_{r_sel}. In FIG. **12**, the sel voltage remains at V_{high_sel} while the tg voltage rises from V_{low_tg} to V_{high_tg} and falls back to V_{low_tg}. In FIG. **12**, the time t_{pw_sel} is the duration during which the tg voltage remains at V_{high_sel}. The sel voltage falls from V_{high_sel} to V_{low_sel} over a time of t_{f_sel}.

The tg voltage rises from V_{low_tg} to V_{high_tg} over a time of t_{r_tg}. In response, the fd voltage also rises. The tg voltage falls back to V_{low_tg} over a time of t_{f_tg}. In response, the fd voltage also falls. The signal level is the difference between this final fd voltage and the fd voltage after the fd voltage falls due to gate coupling with the falling rst voltage.

In FIG. **11**, the sel voltage does not remain at V_{high_sel} while the tg voltage turns high and back low. Instead, after the sel voltage has risen to V_{low_sel} for the first time, the sel voltage falls to V_{low_sel} and after the sel voltage has been at V_{low_sel} for a time delay of t_{gap_2}, the tg voltage begins to rise from V_{low_tg} to V_{high_tg}. After the tg voltage falls from V_{high_tg} to V_{low_tg} and the tg voltage has been at V_{low_tg} for a time delay of t_{gap_3}, the sel voltage begins to rise for a second time from V_{low_sel} to V_{high_sel}. For both sel voltage pulses in FIG. **11**, the sel voltage rises from V_{low_sel} to V_{high_sel} over a time of t_{r_sel}, and the sel voltage falls from V_{high_sel} to V_{low_sel} over a time of t_{f_sel}. For both sel voltage pulses in FIG. **11**, the time t_{pw_sel} begins when the sel voltage begins to rise from V_{low_sel} to V_{high_sel}, and ends when the sel voltage begins to fall from V_{high_sel} to V_{low_sel}.

Both RG and TG are turned ON to reset the PD node, and reset the PD. This ensures to remove all the residual charge from the PD (if any). FIGS. **9** and **10**. Reset is followed by charge integration. Both gates are kept at low voltages while charge is integrated in the PD. At the end of the charge integration, charge readout period starts. This is illustrated in FIGS. **11** and **12**. First, the RG is turned on and the reset level is sampled by turning the Row_sel transistor ON. Then the TG is turned on to transfer the charge to the FD. The Row_sel can be either kept at ON state, or turned ON again to sample the signal level. This operation is repeated every frame time.

Design Methodology:

The pixel layout and implants in this innovation are optimized by a simulation methodology that insures a near optimal solution. An description of this device design flow is provided below:

Step 1: Choose a diode pinning implant. We suggest an implant similar or identical to PLDD as the PD pinning implant.

Pldd implant can be used to pin the surface of the PD with holes to the most negative potential. This insures low dark current and a surface electric field favorable to collection of blue light. Pldd is not the only solution as pinning implant. It is preferred since it comes free with the CMOS process and works well as the pinning implant of the PD. In this innovation the choice of the exact dose and energy for the pinning implant are less critical because the pinning implant position greatly reduces the effect of the electrical barrier to charge transfer. The pinning implant is self aligned to the transfer gate edge like a PLDD which reduces variation due to errors in dimensions and alignment of the mask.

Step 2: Select a TG length depending on the pixel size, layout and architecture.

And select starting dose and energy implants for the Ntype Deep and Ntype shallow ring implants for the photodiode.

Obtain the following by Steady-state analysis:

3) Determine the empty PD potential by adjusting the n-type deep and n-type shallow ring implants to obtain a desired amount of signal capacity with the TG off. If it is too high, charge transfer will suffer. If it is too low, the signal level will be too low.

And then obtain the following by transient analysis:

4) Adjust the TDBI concentration to isolate the charge from the floating diffusion while the TG is OFF. If there is too much leakage, increase the TDBI doping.

5) Find the maximum signal level by overfilling the PD and reaching a steady state over time with the TG turned OFF.

6) Transfer the charge from the PD to floating diffusion by switching the TG ON and OFF. If charge is trapped, raise the TG ON voltage. Adjust the ring implant dose, energy and location to achieve a potential gradient towards the FD during charge transfer. The maximum transfer gate voltage applied in the analysis is based upon the ability to generate and manage an elevated potential in the CMOS process. An example is the use of a 5.5 volt maximum transfer gate voltage for a 3.3 volt CMOS process. (a 3.3 volt CMOS process is a process for which a 3.3 volt potential can be applied across the gate dielectric while maintaining acceptable long term reliability). The goal of the device design is to insure that complete charge transfer occurs below the target maximum voltage to insure margin for manufacture.

7) If the charge cannot be transferred completely or if there is not enough diode capacity after the step, go back to the beginning and repeat the steps, typically starting from 1) to optimize the pixel.

Optimization of the pixel is an iterative process. The convergence to the desired solution is faster if the starting point is not very far off. Therefore, the first guess is important. A good guess based on previous experience makes a good starting point.

After a desired signal capacity is achieved and the pixel operation is verified by simulations, continue with the following analysis:

Color cross-talk:

8) If there is no residual charge in the PD after charge transfer, and the desired signal level is achieved, the color cross-talk should be determined. For this purpose, light at different wavelengths (blue, green, and red) should be shined onto the pixel while extracting the amount of charge collected in the adjacent PD. The p-well provides very good isolation between pixels. The TDBI function as an isolation barrier between pixels should be verified.

9) If the cross-talk is higher than tolerable amount, go back to earlier steps, typically from step 1),

a. adjust the depth of charge collection by changing the n-type PD implant energy and/or

b. use p-well as oppose to the TDBI for STI, and/or

c. make the PD to PD distance larger in the layout.

Sensitivity to the misalignment of mask layers:

10) Move mask layers around to verify the critical dimensions. The pixel operation may be very sensitive to some of the drawn locations of the mask layer. Determine the most crucial layers, and the degree of the failure if the mask is misaligned. Find more robust solutions. A clear advantage of this innovation of the relative insensitivity of the device operation to normal variation in the size and placement of the implant masks.

Embodiments of the TDBI implant cover the left edge of the transfer gate device to provide an adequate barrier and isolation between the floating node (or sense node) and the photodiode. The TDBI concentration is targeted so that the TDBI boron under the gate can be inverted to form an N type channel. This inversion is made facile by the ability to pump the transfer gate to an elevated voltage to continue the charge transfer process as the channel and photodiode potential become more positive. The TDBI implant and the deep phosphorous diode implant overlap. This insures that the right portion of the transfer gate device is electrically coupled to the photodiode.

Features for Device Performance in Integration into CMOS:

1) Use of n-type MOS device in the pixel:

reduces cost and assures predictable performance

p-well implant for CMOS n-type FET provides effective energy barrier for electron cross-talk between pixels.

TDBI also provides a good barrier between the adjacent pixels.

Depending on the layout, both standard and lighter TDBI can be used for isolation.

TDBI can also be used for reset transistor. The threshold voltage of this transistor is reduced and the RG cam be laid out in the same TDBI as the TG.

FIG. 13 sows that if the reset transistor is designed with the p-well, the layout is optimized to integrate with the transfer gate implant 705 insuring optimum separation 160 (~0.3 microns to 0.5 microns) between the higher doped NMOS p-well Edge 708 and the lower doped TDBI 705. Thus separation refers to the implantation

areas. After thermal processing steps, the implanted dopants diffuse closer, shrinking or eliminating the gap.

In our innovation adjustable voltages of increased absolute potential are also provided for the gate of the reset transistor. This insures that the sense node potential can be reset to the power supply voltage of the chip to insure maximum pixel capacity.

These two different devices with different functions and required doping profiles of silicon impurities are integrated to be in very close proximity to support pixel scaling.

However, in shared pixel designs this approach affords room to use a more conventional NMOS p-well for the transfer gate device. There is sufficient room for the NMOS device p-well edge to be separated from the Right edge of the Transfer device.

The high concentration of the p-well for NMOS transistors has decreased to within ½ order (about a factor of 3.2) of the wafer background doping before reaching regions of TDBI doping.

2) Transfer Device Barrier Control Boron Implant

Boron implant for control of barrier potential for charge transfer from floating diffusion node/reset node with the following features:

Implant is not centered on the channel formed by the intersection of the transfer gate poly and active but is moved away from the n-type photodiode region. The shift is determined by the charge transfer operation. For one embodiment, the TDBI overlaps with the TG by 0.2 um. (FIG. 14). The top view of the layout for the non-shared embodiment of the pixel is shown in FIG. 15. Charge transfer occurs at the floating node edge of the transfer gate, very close to the silicon surface. This shift insures the best barrier properties to transfer the charge.

FIG. 14 is a cross-sectional schematic of a pixel. The pixel is formed in a <100> substrate 700 with a p-type doping of 5×10^{14} cm^{-3}. Shallow trench isolation 702 separates a photodiode formed from implants (N-type deep implant 715 and N-type ring implant 712) from an adjacent photodiode 790. There is a separation between the transfer device barrier implant 705 and the reset transistor p-well 716 (in this example, with a separation of about 0.3 um-0.5 um), and an overlap of the transfer device barrier implant 705 with the transfer gate 717 (in this example, with an overlap of about 0.2 um). The transfer gate 717 also overlaps the floating diffusion 720 and the photodiode. The transfer gate 717 is aligned with the p+ pinning implant 723. The floating diffusion 720 is formed to be positioned partly in the transfer device barrier implant 705 and partly in the reset transistor p-well 716. The reset gate 716 overlaps the n+ floating diffusion 720 and the n+ RD 730.

FIG. 15 is a plan view schematic of a pixel. The pixel is formed with a separation 160 between the transfer device barrier implant 125 and the reset transistor p-well implant 120, and an overlap of the transfer device barrier implant 125 with the transfer gate 152. Also shown are NMOS transistor gates 145, photodiode area 143, and active outline 140.

TDBI doping is process dependent, for example boron with dose and energy in the range of 1e12, 40 keV to 5e13, 250 keV.

The Doping level for the barrier is optimized in concert with the implants for the photodiode n type region to insure optimum capacity, built in anti-blooming control, and full charge transfer to insure true CDS and low noise.

3) Ring and Core Implants for n-type photo collection region. (Photodiode area)

The capacity and charge transfer and noise are optimized in CMOS integration through the use of two implants to define the n-type area and ensure optimum integration into CMOS.

A low dose phosphorous implant with dose in the range of 1e12 to 1e13 and energy in the range of 200 keV to 37 keV.

This phosphorous implant provides optimum depth for the photodiode electric field to ensure low cross talk and high collection of red light.

A second ring-shaped phosphorous implant (FIG. 16) is placed around the perimeter of the device and in intimate contact with the transfer channel implant to maximize the capacity of the pixel in a CMOS context while providing a favorable electric field. This concept is used in conjunction with the TDBI and p-well isolation in CMOS with STI. The width of this implant is determined in one embodiment as about 0.5 um. The effect of this implant starts to disappear as it becomes narrower. The misalignment and control of the width also become more difficult. If it is laid out wider, the maximum of the potential becomes flatter and shifts towards the PD center.

FIG. 16 is a plan view schematic of a pixel, similar to FIG. 15. The photodiode area 143 is characterized by an n-type diode ring implant 320. Cross-section 1600 for the 2D simulation is indicated.

Best dose and energy for the phosphorous ring implant is in the range of 5e11 to 1e13 and 50 keV to 250 keV.

The optimum dose and energy for the Phosphorous implant is determined by process and device simulations as explained in the design methodology. Cross-sectional view is shown in FIG. 32. The fabrication process is shown in FIGS. 17-31.

In FIG. 17, shallow trench isolation 702 and SiO₂ 701 are formed on p-type substrate 700. FIG. 18 shows the patterning 703 and implantation 704 of the transfer device barrier implant. FIG. 19 shows the transfer device barrier implant 705.

FIG. 20 shows the patterning 706 and implantation 707 of a typical p-well implant. FIG. 21 shows the p-well implant 708 for the signal and reset transistors and isolation 709 of neighboring photodiodes.

FIG. 22 shows the patterning 710 and implantation 711 of the photodiode ring implant. FIG. 23 shows the photodiode ring implant 712.

FIG. 24 shows the patterning 713 and implantation 714 of the photodiode deep implant. FIG. 25 shows the photodiode deep implant 715.

FIG. 26 shows the patterning and growth of the gate oxide and patterning and deposition of the polysilicon gates 716 and 717.

FIG. 27 shows the patterning 718 and implantation 719 of the nldd, or floating node. FIG. 28 shows the patterning 721 and implantation 722 of the pldd, or pinning implant. FIG. 29 shows annealing (The nldd or n+ floating diffusion 720 and the pldd or p+ pinning layer 723 are shown) and the growth of the transistor spacers 724.

FIG. 30 shows the patterning 725 and implantation 726 of the sources and drains of the transistors. FIG. 31 shows the annealing.

4) Work Function Control of Transfer Device Gate

The barrier of the transfer gate is optimized by using a polycrystalline silicon gate with a more p-type work function, resulting in improved properties. This increase in

barrier properties allows improved overall performance when combined with a voltage boost on the transfer gate during the on state. The higher work function makes the off state more "OFF" without the use of higher doping levels and attracts holes to the silicon surface under the TG (pinning), reducing dark current via electron-hole recombination. The increased barrier can then be easily overcome by a controlled voltage applied to the transfer gate during the on or charge transfer state.

There is also a significant reduction of the dark current by using a pinned PD rather than a normal pn diode. The pinned PD keeps the surface accumulated by holes, and therefore any electron that becomes free due to surface interface states recombines with the hole immediately, and the dark current is eliminated. The silicon under the TG area with the existing structure remains depleted during operation. This area still contributes to dark current generation which can be eliminated by changing the poly doping to p-type.

The TG in some embodiments uses an n-type poly. With typical operating voltages of the CMOS process, the area under the TG remains depleted and generates dark current.

There are other solutions to this problem such as applying a negative voltage to the TG and attracting holes to the surface while the gate is OFF. This requires additional negative bias voltage which is more complex to create and manage.

Using p-type poly gate instead of n-type poly gate for the TG: The work-function difference between the p-type poly to the substrate acts like negative biasing and attracts holes to the surface. By making the TG polycrystalline silicon p-type, the dark current generation under the TG is eliminated during the charge collection period.

The work function of the gate can also be sloped to be non-constant with the work function over the n-type area being more p-type than the work function over/near the sense node.

A charge transfer device with a more p-type work function is achieved by: blocking n-type doping normally applied to NMOS type devices, and/or applying p-type doping which is also used for surface pinning, and/or adding additional p-type implants such as a special o-type implant, PLDD or p+ implant.

One embodiment for small pixels dopes the poly p-type with a special mask after polycrystalline silicon deposition and before patterning. Suitable polycrystalline silicon etch should be obtained with the p-type doping present in the CMOS process baseline.

FIG. 33 illustrates the p-type poly TG 717 and the silicon under the gate while it is on OFF state. The charge integration period is usually much longer than the charge transfer period. Thus, pinning the silicon under TG will eliminate the dark current generation in this region almost completely. This region will be in depletion only for a short period of time during charge transfer. The dark current generation during this time is negligible.

5) Adaptive Circuitry—Blooming Control—Incomplete Charge Transfer

Blooming Control during charge integration: Because the transfer gate's voltage is variable, it can be used for blooming control during charge integration. If there is excessively bright light, there will be excess charge in the PD. This excess charge should rather be drained to the floating diffusion node of the same pixel rather than cause blooming to occur in the neighboring pixels. If the light level is so high that there will be blooming in the adjacent pixels, the TG voltage should be lowered, to enable the excess charge to flow to the floating diffusion node easily. This voltage is

variable and can be is adjusted to the desired level by the on-chip adaptive circuitry. (FIG. **5**)

Charge Transfer: The same gate voltage is used differently, in the case of incomplete charge transfer from the PD to the floating diffusion during the charge transfer period. The TG voltage should be increased by an on-chip charge pump. The charge pump provides voltages at least a threshold voltage of the n-type MOS transistor (VT) above the supply voltage or higher. This gate operates under a strong backbias condition. Therefore, it can handle relatively high voltages. This feature provides extra margin for the charge transfer. (FIG. **8**).

6) Optimization of starting material

Optimum integration of the advanced pixel occurs when the CMOS starting material is chosen to be low doped p on p+ epi. The use of p+ epi eliminates latch up concerns that might otherwise arise from any significant change in the substrate concentration.

The doping level should be as low as practical with acceptable control in the manufacturing process and is recommended to be in the range of 2E14 to a maximum of 1E15. This low doping allows the best optimization of the charge transfer and allows the electric fields for charge collection to extend as deeply as possible into the silicon. One embodiment has about 4E14 Boron doping.

The thickness of the lightly doped surface layer should be optimized to allow the best possible light collection. The choice of a thick epi layer improves light collection for the red but increases cross talk and increases the potential for latch up. Use of a thin layer will interfere with CMOS n-well and p-well doping and results in reduced light collection in the red.

The optimum EPI thickness is in the range of 4 to 7 microns. (FIG. **34**).

FIG. **34** is a cross-sectional schematic of a photodetector of a pixel. The p+ epitaxial layer having a low concentration layer **530** having a thickness **520** is formed on p+ layer of substrate **510**. The N-type photodiode **550** is formed in the layer **530**.

7) Pixel layout

Contacts to polysilicon that are over the active channel are shown in FIG. **35**. The placement of contacts over the pixel channel allows the pixel layout to be smaller with a higher fill factor and better performance.

8) Dark current reduction through use of PLDD implant to isolate the photodiode from the surface states.

The use of the PLDD implant as the p-type surface pinning implant saves one mask and works well. This implant pins the surface to the most negative voltage in the device and keeps the surface accumulated by holes. In addition, as explained above, the region under the TG can be pinned by doping this gate p-type. This region is depleted only during charge transfer period, which is typically much shorter than the charge integration period. Thus, the PD surface is pinned, and the dark current generation is eliminated.

9) Correlated Double Sampling (CDS) and Very Low Noise improve low-light performance.

Due to surface pinning in the PD, the dark current shot noise becomes very low. The other major noise component is the kTC noise in the pixel. With the 3 transistor pixels, a true CDS cannot be done. Embodiments of the pixel design enable a true CDS by holding the charge isolated in the PD region. The FD potential is sampled twice, before and after the charge transfer. The difference of these levels is due to the signal integrated in the PD. Subtracting the signal level from reset level eliminates the kTC noise.

As the noise level is reduced the low-light performance of the imager is improved. This is very important for the digital still camera applications.

10) Shared Pixel Architecture

The shared pixel schematic is shown in FIG. **2**, and the layout in FIG. **35**. This pixel works fine in a single pixel architecture. However, it is also very suitable for a shared architecture because the transfer gates can be laid out very symmetrically and be surrounded by the TDBI, while the reset gate, source-follower and row-select transistors are laid out in the p-well next to the photodiodes. It becomes also very simple to lay out the deep PD n-implant and p+– pinning implant to cover all 4 PDs at once.

When the charge integration period is over, the TGs turn ON one by one, transferring the charge from the PD to the floating diffusion node. The charge transfer occurs in the vertical direction for all the PDs and is very symmetrical. The TGs are laid out as very simple gate structures to avoid 3D effects, especially caused by corners. The accumulated charge does not need to turn any corners and change direction with this layout, and flows vertically in one dimension.

The four PDs in the shared architecture are surrounded by the TDBI for isolation. The TDBI is also used as a barrier layer between them. The active devices (Reset transistor, Source Follower and Row-select transistors) are laid out in the p-well.

The layout becomes more efficient by

putting all the PDs together and isolating them with the TDBI, and

sharing the active transistors that are laid out in the p-well.

About 30% . . . 40% higher fill factor is achieved compared to single pixel architecture.

FIG. **36** is a simplified block diagram of a computer system **3610** suitable for use with embodiments of the present invention. Computer system **3610** typically includes at least one processor **3614** which communicates with a number of peripheral devices via bus subsystem **3612**. These peripheral devices may include a storage subsystem **3624**, comprising a memory subsystem **3626** and a file storage subsystem **3628**, user interface input devices **3622**, user interface output devices **3620**, and a network interface subsystem **3616**. The input and output devices allow user interaction with computer system **3610**. Network interface subsystem **3616** provides an interface to outside networks, including an interface to communication network **3618**, and is coupled via communication network **3618** to corresponding interface devices in other computer systems. Communication network **3618** may comprise many interconnected computer systems and communication links. These communication links may be wireline links, optical links, wireless links, or any other mechanisms for communication of information. While in one embodiment, communication network **3618** is the Internet, in other embodiments, communication network **3618** may be any suitable computer network.

User interface input devices **3622** may include a keyboard, pointing devices such as a mouse, trackball, touchpad, or graphics tablet, a scanner, a touchscreen incorporated into the display, audio input devices such as voice recognition systems, microphones, and other types of input devices. In general, use of the term "input device" is intended to include all possible types of devices and ways to input information into computer system **3610** or onto computer network **3618**.

User interface output devices **3620** may include a display subsystem, a printer, a fax machine, or non-visual displays such as audio output devices. The display subsystem may

include a cathode ray tube (CRT), a flat-panel device such as a liquid crystal display (LCD), a projection device, or some other mechanism for creating a visible image. The display subsystem may also provide non-visual display such as via audio output devices. In general, use of the term "output device" is intended to include all possible types of devices and ways to output information from computer system **3610** to the user or to another machine or computer system.

Storage subsystem **3624** stores the basic programming and data constructs that provide the functionality of certain embodiments of the present invention. For example, the various modules implementing the functionality of certain embodiments of the invention may be stored in storage subsystem **3624**. These software modules are generally executed by processor **3614**.

Memory subsystem **3626** typically includes a number of memories including a main random access memory (RAM) **3630** for storage of instructions and data during program execution and a read only memory (ROM) **3632** in which fixed instructions are stored. File storage subsystem **3628** provides persistent storage for program and data files, and may include a hard disk drive, a floppy disk drive along with associated removable media, a CD-ROM drive, an optical drive, or removable media cartridges. The databases and modules implementing the functionality of certain embodiments of the invention may be stored by file storage subsystem **3628**.

Bus subsystem **3612** provides a mechanism for letting the various components and subsystems of computer system **3610** communicate with each other as intended. Although bus subsystem **3612** is shown schematically as a single bus, alternative embodiments of the bus subsystem may use multiple busses.

Computer program medium **3640** can be a medium associated with file storage subsystem **3628**, and/or with network interface **3616**. The computer program medium can be an optical, magnetic, and/or electric medium that stores circuit data such as a layout, a tapeout, or other design data.

Computer system **3610** itself can be of varying types including a personal computer, a portable computer, a workstation, a computer terminal, a network computer, a television, a mainframe, or any other data processing system or user device. Due to the ever-changing nature of computers and networks, the description of computer system **3610** depicted in FIG. **36** is intended only as a specific example for purposes of illustrating the preferred embodiments of the present invention. Many other configurations of computer system **3610** are possible having more or less components than the computer system depicted in FIG. **36**.

While the present invention is disclosed by reference to the preferred embodiments and examples detailed above, it is to be understood that these examples are intended in an illustrative rather than in a limiting sense. It is contemplated that modifications and combinations will readily occur to those skilled in the art, which modifications and combinations will be within the spirit of the invention and the scope of the following claims.

What is claimed is:

1. A method of designing with a simulation a CMOS image sensor integrated circuit having a photodetector using energy of photons reaching the photodetector to excite electrons; a transfer device with a first terminal coupled to the photodetector, a second terminal coupled to the corresponding node, and a control terminal causing a transfer of the electrons from the first terminal to the second terminal in response to receiving a control signal of sufficient value; a p-type region having a concentration stronger than a back-

ground concentration and having a lateral position at least partly under the control terminal of the transfer device; the simulation comprising:

selecting design parameters of a surface p-type region laterally positioned at the photodetector;

selecting design parameters of the transfer device;

selecting design parameters for a first n-type region and a second n-type region of the photodetector, the first n-type region at a first depth range in the integrated circuit and receiving the electrons excited by the photons, and the second n-type region at a second depth range wherein the first depth range includes depths deeper than the second depth range, the second n-type region being adjacent to the first n-type region and receiving the electrons from the first n-type region;

selecting design parameters of the p-type region;

filling the photodetector with electrons to a maximum capacity;

verifying that the maximum capacity of the photodetector meets a design specification of the integrated circuit; and

verifying that raising the control voltage on the control terminal, without exceeding a voltage tolerance of a dielectric, transfers the electrons from the photodetector to the corresponding node to be measured and removed.

2. The method of claim **1**, wherein the surface p-type region is self-aligned to the control terminal of the transfer device.

3. The method of claim **1**, wherein the surface p-type region pins a Fermi level of a surface of the photodetector.

4. The method of claim **1**, further comprising:

repeating said selecting design parameters of the surface p-type region, the transfer device, the first n-type region, the second n-type region, the p-type region, and said filling the photodetector with electrons to a maximum capacity, until said verifying of the maximum capacity of the photodetector is successful.

5. The method of claim **1**, further comprising:

repeating said selecting design parameters of the surface p-type region, the transfer device, the first n-type region, the second n-type region, the p-type region, and said filling the photodetector with electrons to a maximum capacity, until said verifying that raising the control voltage transfers the electrons is successful.

6. The method of claim **1**, further comprising:

shining the photons corresponding to multiple wavelengths on the photodetector; and

verifying sufficient isolation at the multiple wavelengths between the photodetector and a neighboring photodetector.

7. The method of claim **1**, wherein the plurality of signal devices includes a plurality of row select transistors coupled to the row and column circuitry and a plurality of source follower transistors coupled to the plurality of nodes.

8. The method of claim **1**, wherein the plurality of photodetectors is a plurality of photodiodes.

9. The method of claim **1**, wherein each measurement of the total of the photons is corrected by correlated multiple sampling with a prior measurement of the total of the photons.

10. A computer readable algorithm designing a CMOS image sensor integrated circuit having a photodetector using energy of photons reaching the photodetector to excite electrons; a transfer device with a first terminal coupled to the photodetector, a second terminal coupled to a corresponding node, and a control terminal causing a transfer of

the electrons from the first terminal to the second terminal in response to receiving a control signal of sufficient value; a p-type region having a concentration stronger than a background concentration and having a lateral position at least partly under the control terminal of the transfer device; the computer readable algorithm performing:

selecting design parameters of a surface p-type region laterally positioned at the photodetector;

selecting design parameters of the transfer device;

selecting design parameters for a first n-type region and a second n-type region of the photodetector, the first n-type region at a first depth range in the integrated circuit and receiving the electrons excited by the photons, and the second n-type region at a second depth range wherein the first depth range includes depths deeper than the second depth range, the second n-type region being adjacent to the first n-type region, and receiving the electrons from the first n-type region;

selecting design parameters of the p-type region;

filling the photodetector with electrons to a maximum capacity;

verifying that the maximum capacity of the photodetector meets a design specification of the integrated circuit; and

verifying that raising the control voltage on the control terminal, without exceeding a voltage tolerance of a dielectric, transfers the electrons from the photodetector to the corresponding node to be measured and removed.

11. The computer readable algorithm of claim 10, wherein the algorithm is carried by an electromagnetic waveform.

12. The computer readable algorithm of claim 10, wherein the algorithm is carried by an optically accessed storage medium.

13. The computer readable algorithm of claim 10, wherein the algorithm is carried by a magnetically accessed storage medium.

14. The computer readable algorithm of claim 10, wherein the plurality of signal devices includes a plurality of row select transistors coupled to the row and column circuitry and a plurality of source follower transistors coupled to the plurality of nodes.

15. The computer readable algorithm of claim 10, wherein the plurality of photodetectors is a plurality of photodiodes.

16. The computer readable algorithm of claim 10, wherein each measurement of the total of the photons is corrected by correlated multiple sampling with a prior measurement of the total of the photons.

17. A set of masks for a CMOS image sensor integrated circuit having a photodetector using energy of photons reaching the photodetector to excite electrons; a transfer device with a first terminal coupled to the photodetector, a second terminal coupled to the corresponding node, and a control terminal causing a transfer of the electrons from the first terminal to the second terminal in response to receiving a control signal of sufficient value; a p-type region having a concentration stronger than a background concentration and having a lateral position at least partly under the control terminal of the transfer device; the set of masks designed by a simulation algorithm performing:

selecting design parameters of a surface p-type region laterally positioned at the photodetector;

selecting design parameters of the transfer device;

selecting design parameters for a first n-type region and a second n-type region of the photodetector, the first n-type region at a first depth range in the integrated circuit and receiving the electrons excited by the photons, and the second n-type region at a second depth range wherein the first depth range includes depths deeper than the second depth range, the second n-type region being adjacent to the first n-type region, and receiving the electrons from the first n-type region;

selecting design parameters of the p-type region;

filling the photodetector with electrons to a maximum capacity;

verifying that the maximum capacity of the photodetector meets a design specification of the integrated circuit; and

verifying that raising the control voltage on the control terminal, without exceeding a voltage tolerance of a dielectric, transfers the electrons from the photodetector to the corresponding node to be measured and removed.

*   *   *   *   *